Proceedings World Geothermal Congress 2023
Beijing, China, October 9-11 2023

Detecting geothermal anomalies in the NE of Morocco using Landsat 8 thermal infrared remotely sensed data

Redouane Meryem[1], Haissen Faouziya[1], Sadki Othman[2], Raji Mohammed[1], Si Mhamdi Hicham[3], Khalis Hind[4]

1: Faculty of Sciences Ben M'sik, Casablanca, 20000, Morocco (*meryem.redouane.2015@gmail.com*)

2: National Office of Hydrocarbons and Mines, Rabat, Morocco

3: Faculty of Sciences and Techniques, Errachidia, Morocco

4: Faculty of Sciences Dhar El Mahraz, Fez, Morocco

Keywords: Remote sensing, Landsat-8 OLI/TIRS, LST, geothermal anomalies

ABSTRACT

In the last few years, Remote sensing information attracted a wide range of interest among researchers in different disciplines. Investigation of renewable energy resources worldwide, especially for geothermal exploration was not an exception. In contrast to geophysical methods, the use of Remote sensing tools allow us to target a larger-scale area for thermal exploration, by working on thermal infrared imagery (TIRS) to acquire surface temperatures and identify thermal anomalies. This study investigates the geothermal potential of Northeast of Morocco, where the heat flow is significantly high and the geothermal gradient is of 129 °C/km. It also highlights the different geothermal anomalies for future studies and development.

Land Surface Temperature (LST) is known as one of the indicators of the heat flow; however, the latter is not the only parameter that implies the changes on it, the meteorological conditions together with the altitude contribute in the result as well. Thus, we analysed LST derived from Landsat-8 OLI/TIRS of warm seasons of each year between 2016 and 2021, and used all other available data to evaluate the results. Although the produced map shows certain limitations, the result depicts correctly most of areas with high geothermal potential (zones with hot springs or wells Temperatures) and appear to correlate well with the fault trending system. We approve of the great effectiveness of TIRS remote sensing as an economic tool for geothermal mapping.

1. INTRODUCTION

Undoubtedly, climate change situation has led to many debates regarding the current situation of the high-energy consumption and non-renewable resources used to cover the human`s modern lifestyle. This situation has lately imposed the transition from fossil fuels to other clean and renewable energy resources, among these green resources, there is geothermal energy, and its use is increasing through the years. Geothermal exploration is generally pricey and requires many field surveys; these conditions make the exploration very limited in both spatial and financial aspects.

During the last few years, remote sensing has become a valuable tool for geoscientists in different topics and disciplines (Geography, Geomorphology, Structural geology etc.). Remote sensing can also be used to detect geothermal anomalies with high accuracy, as it was concluded by many authors (i.e. van der Meer et al., 2014; Chan et al., 2017; Gemitzi et al., 2021), using different techniques, involving remotely sensed data. These authors used Landsat images (namely Landsat 7 ETM+ and Landsat 8 (OLI/TIRS)) and calculated or derived the LST (Land Surface Temperatures) from thermal bands (100 m, resampled to 30 m). Consequently, they referred to thermal infrared data (TIRS) as a cost-effective technique as their results were satisfying and areas with high geothermal potential were consistent with the faults pattern responsible for heat transfer from heat sources. However, several restrictions may affect the accuracy of the LST result, such as topography, land cover in addition to natural conditions and events (Chan et al., 2017; Romaguera et al., 2018), which can be easily overcome after applying some corrections.

The aim of the present work is to identify capital geothermal areas in Nador-Berkane region in northeast of Morocco, based on the compilation of different relevant data (LST, soil moisture, thermal waters temperatures, weather stations, faults and hydro pattern) during the warm season of the years between 2016 and 2021, using Landsat 8 (OLI/TIRS).

2. GEOLOGICAL SETTINGS

Morocco is located in the north westernmost part of Africa, limited in the north by the Mediterranean Sea, in the south by Mauritania, in the east by Algeria and in the west by the Atlantic Ocean. The country has been affected by the Alpine Orogeny, and the collision between Eurasian and African plates printed the area with many volcanic manifestations, some of them are sync-collision, while others are post-collision manifestations (Maury et al., 2000; Coulon et al., 2002). Most of the volcanic centres are aligned NE-SW, from Nador and Melilla region in the Rif to Agadir region in the Anti-Atlas (Figure 1), which has led some authors (Missenard and Cadoux, 2006) to suggest the existence of a hot line, usually referred to as the "Moroccan Hot Line".

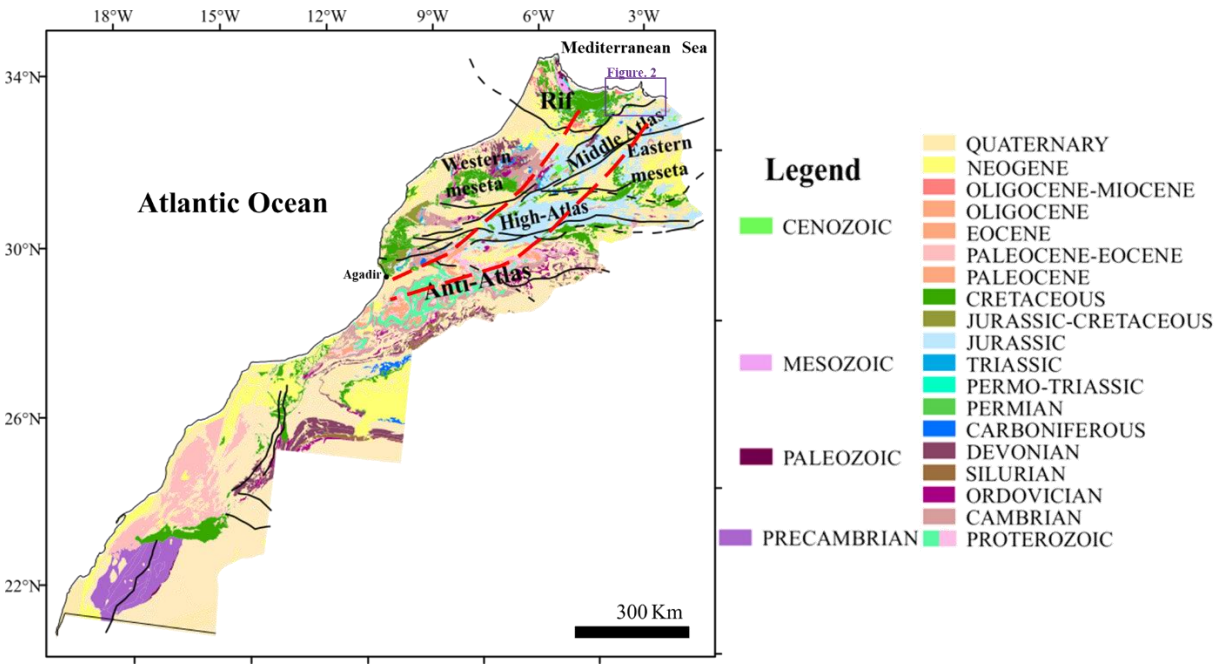

Figure 1: Regional geological settings. Red dotted line represents the Hot Line suggested by (Missenard and Cadoux, 2006)

Northeastern Morocco consists of several structural zones, which can be grouped as the eastern part of the Rif belt, its foreland and the eastern meseta (Middle-Atlas) (Figure 2). The eastern Rif is located in the east of areas that have undergone latitudinal distortions associated with the movement of the Alboran block and it consists of several depressions (i.e. Kert, Ghareb plains, Melilla…), individualized during the Upper Tortonian-Messinian and Pliocene, and which are separated by the voclanic massif of Beni Bou Ifrour and Gourougou volcanic complex (Figure 2). They are limited in the NW by the Temsamane and other external Riffian units and in the South by the Ghareb-Kebdana chain (Figure 2). These structural units exhibit some paleogeographic changes, especially during the Middle-Upper Lias and Dogger, while major faults replayed permanently (Mattauer et al., 1977; Rakus, 1979).

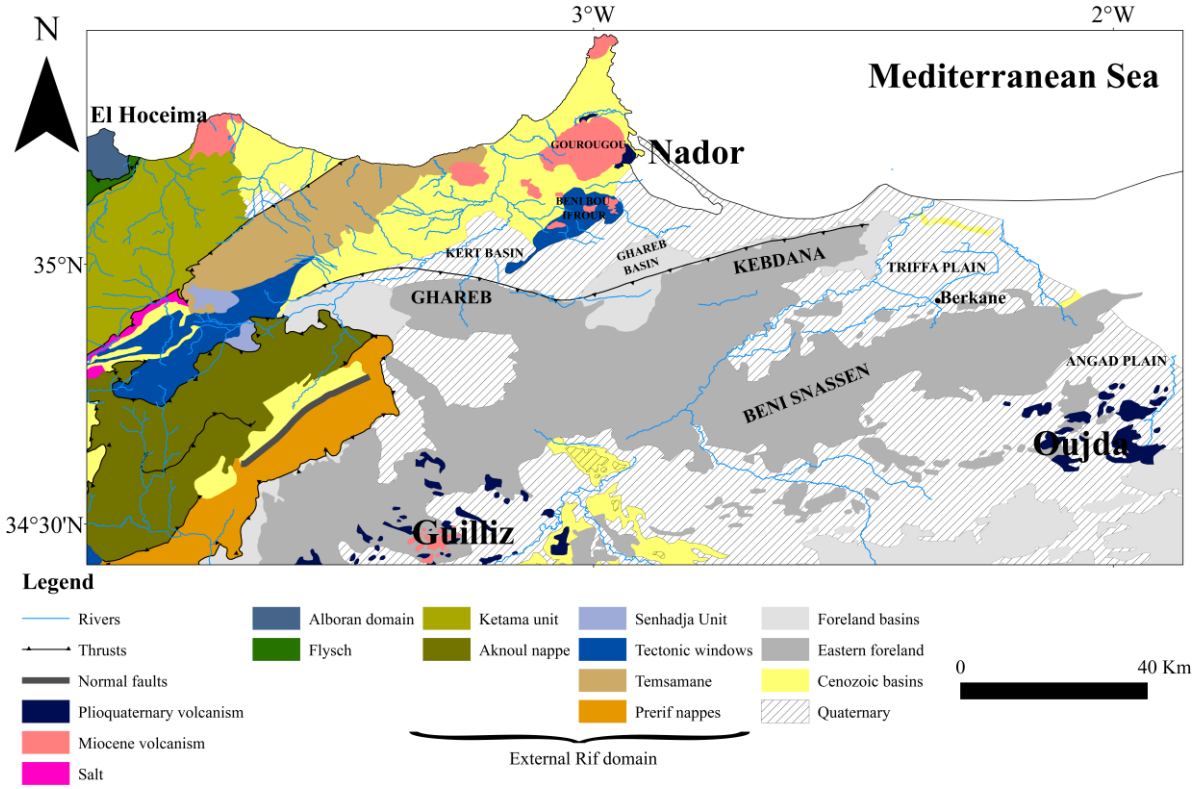

Figure 2: Geological map of Eastern Rif (Morocco) with the distribution of volcanism in the Neogene basin, after Suter, 1980.

NE of Morocco is characterized by a recent tectonic framework, from which emerge major orientations NE-SW (ranging from N40 to N70); N-S (ranging from N10 to N45); and EW to WNW-ESE (ranging from N80 to N120) (Redouane et al., 2022). Miocene volcanic activity within the study area resulted in some shoshonitic eruptions, between 8 and 4.5 Ma and some calcalkaline eruptive centres between 6.2 and 4.8 Ma (Hernandez and Bellon, 1985). Later on, an alkaline episode has took place between 6 and 0.8 Ma

(El azzouzi et al., 1999). Northeast of Morocco is also known by the abundance of hot springs, a high Heat Flux (Figure 3), a geothermal gradient of 50 ºC/km and high residual magnetic anomalies (Rimi 1999; Zarhloule et al., 2010). Sedimentary reservoirs feeding thermal springs have great thickness. They belong to the Atlas domain and consist of Liassic limestones (Barkaoui et al., 2013).

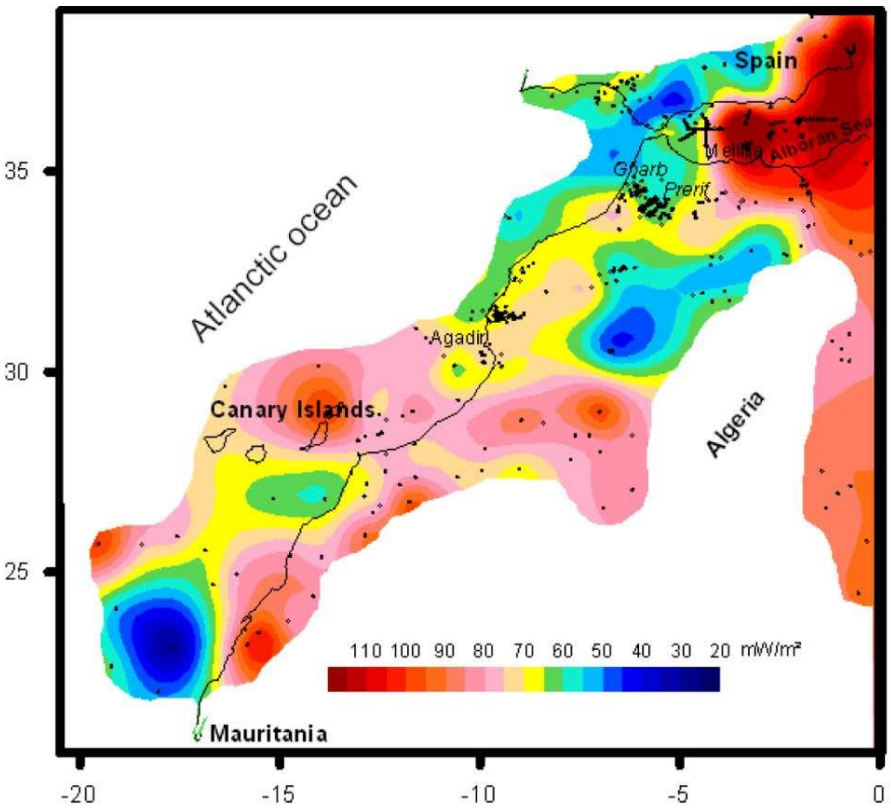

Figure 3: Terrestrial heat flux of Morocco and neighbouring regions (Rimi, 1999)

3. DATA AND METHODS

Acquired spatial images usually require atmospheric correction to fix possible geometric distortions by eliminating existing disturbances due to the presence of gases and dust in the atmosphere that can absorb light.

With the aim of detecting areas with high geothermal anomalies using LST from both Landsat and MODIS, we extracted a 6-year summer time series of LST using Landsat 8 thermal data (USGS, 2022) and a 4-year summer time series MODIS LST (Table 1).

Table 1: Description of the data set

Data	Time Period	Temporal resolution	Spatial resolution
Landsat 8	28th August 2016	16 days	
Band 4 - Red	30th September 2017		30 m
Band 5 - Near Infrared (NIR)	15th June 2018		30 m
Band 10 - Thermal Infrared (TIRS) 1	5th August 2019		100m resampled with cubic convolution at 30m
	6th July 2020		
	23rd June 2021		
MODIS (MOD11A1)	9th August 2017	Daily	1 Km
Land Surface Temperature / Emissivity Daily L3 Global 1 km	15th June 2018		
	6th July 2020		
	23rd June 2021		

To calculate LST we tried two methods; the first involves only the thermal bands (Donglian, 2007; Freitas et al., 2013; Khalis et al., 2021) and the second requires other calculations such as NDVI and emissivity index (Gemitzi et al., 2021). Both methods gave the same results. Therefore, we decided to proceed with the first method and calculate the brightness temperatures (Figure 4).

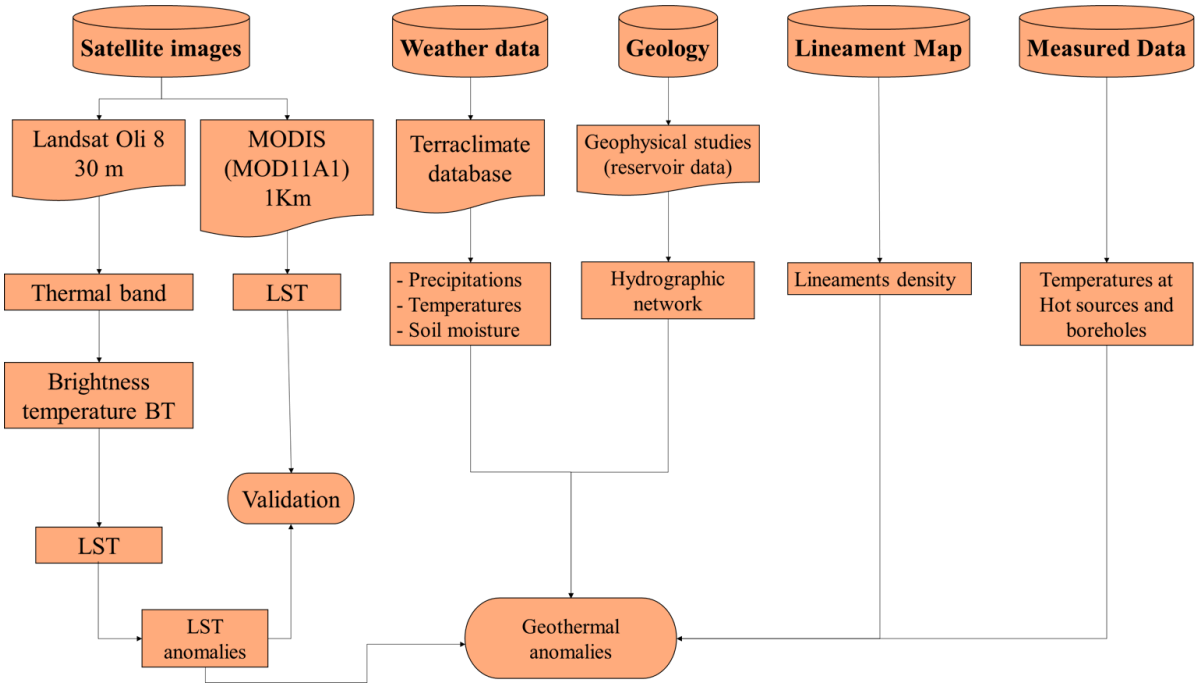

Figure 4: Flowchart of the proposed methodology

Following the reading of the unprocessed images, a preprocessing phase was necessary for a generalized and systematic analysis. The pre-treatment applied to the images included the following procedures:

- Radiometric calibration and rapid radiometric correction

- Atmospheric line-of-sight analysis of hypercubes (FLAASH).

Brightness Temperature

The effective brightness temperature at the sensor (BT) also known as the blackbody temperature is obtained from the spectral radiance using the inverse Plank function (Ronald, 2005).

Conversion of the Digital number (DN) to spectral radiation Lλ (Afrasiabi Gorgani et al., 2013) is done using the following equation:

$$L_\lambda = L_{MIN} + (L_{MAX} - L_{Min}) \times {DN}/{255} \qquad \textit{Eq. 1}$$

With:

Lλ= spectral Radiance,

LMIN= Spectral radiance of DN value

LMAX= Spectral Luminance Value DN 255 DN=Digital number

Conversion of spectral radiance to temperature in Kelvin is done using the following equation (Tucker et al., 1997 ; Afrasiabi Gorgani et al., 2013):

$$B_T = {K_2}\Big/{ln\left(\left({K_1}/{L}\right)+1\right)} \qquad \text{Eq. 2}$$

With:

K1= Calibration constant 1

K2= Calibration constant 2

BT= Surface temperature

Calibration constants K1 and K2 obtained from the Landsat data are reported in Table 2.

Table 2: Calibration constants K1 et K2

Image	Bands	K_1 (w/(m² sr µm)	K_2 (K)
Landsat 8 OLI	Band 10	774.88	1321.08
	Band 11	480.89	1201.14

Temperature can then be converted from Kelvin to Celsius using the following equation:

$$\boldsymbol{B_T = B_T - 273.15} \qquad \text{Eq. 3}$$

In general, surface temperature in Morocco varies from 16 °C/km to 42 °C/km. A mandatory step before any geothermal investigation is to study the variation of temperature.

Validation of Landsat 8 LST against MODIS LST daytime was used in several studies (i.e. Gemitzi et al., 2021) and proved to be of a great effectiveness with a correlation coefficient between 0.8 and 0.9, with Landsat 8 LST demonstrating the higher values. We therefore chose to use it for validation. We used MODIS Terra, Aqua Collection 4 MODIS LST (MOD11A1), we tried to use it for all the six years but we failed to get a clear image for the summer time of the years 2016 and 2019, so we chose to not use them and compare with those of the four other years instead. The validation process also included comparing MODIS LST and Landsat LST with measured temperatures in 18 weather station all over the study area between the years 2016 and 2021 (Table 3).

Table 3: Weather stations data for max and min temperature (°C) between the years 2016 and 2021 (Terraclimate)

Year	2016		2017		2018		2019		2020		2021	
station	Tmax	Tmin	Tmax	Tmin	Tmax	Tmin	Tmax	Tmin	Tmax	Tmin	Tmax	Tmin
34.7185N-2.7047W	30,70	6,50	31,60	3,10	31,10	3,10	31,40	4,50	32,00	4,00	32,10	5,60
34.9251N-2.3256W	31,00	8,20	32,00	5,30	31,7	5,5	31,70	6,50	32,20	6,10	32,00	7,70
34.9264N-3.1538W	31,3	7,9	32,20	4,30	31,9	4,5	31,8	5,8	32,2	5,4	31,60	6,70
34.9309N-2.7427W	30,90	8,70	31,70	20,90	31,50	5,50	31,60	6,60	31,90	6,10	31,70	7,60
34.9849N-2.3584W	31,30	8,50	32,20	5,60	32	5,8	32	6,9	32,30	6,50	32,30	8,10
35.0450N-3.3182W	31,4	8	32,2	4,5	32	4,7	31,6	6	32,2	5,6	31,6	6,7
35.0744N-2.9332W	30,5	9,5	31,4	6,2	31,2	6,4	31	7,6	31,4	10,1	30,8	8,4
35.0810N-2.5187W	31,4	8,2	32,3	5	32,1	5,1	32	6,4	32,3	6	32,1	7,2
35.0985N-2.2812W	31,7	8,6	32,6	6,3	32,5	6,5	32,3	7,7	32,7	7,2	31,9	8,4
35.1072N-2.7288W	31,3	9,8	32,1	6,4	32	6,7	31,8	7,9	32,2	7,3	31,8	8,5
35.1308N-3.1364W	30	9	30,8	5,5	30,7	5,8	30,2	7,1	30,8	6,5	30,1	7,5
35.1328N-2.4213W	31,8	9,2	32,7	6,6	32,6	6,6	32,3	8,1	32,8	7,6	31,9	8,5
35.2086N-2.932W	30,4	9,2	31,2	5,9	31,3	5,9	30,6	7,5	31,3	6,7	30,2	7,7
35.2945N-3.0618W	30,8	9,6	31,6	6,2	31,5	6,2	30,7	7,9	31,4	7,2	30,4	8

35.2472N-3.148W	30,4	9,4	31,2	6,1	31,2	6,2	30,4	7,7	31,1	7,1	30,2	7,9
35.3955N-2.9727W	30,5	9,2	31,3	5,8	31,3	5,8	30,5	7,4	31,2	6,8	30	7,4
35.2217N-2.995W	30,8	7,1	31,6	3,6	31,6	3,6	30,9	5,2	31,5	4,3	30,7	5,4
35.0115N-2.6499W	30,7	7,3	31,5	3,9	31,4	4	31,3	5,3	31,6	4,8	31,5	6,2

4. RESULTS AND DISCUSSION

The present work is based on the hypothesis that geothermal areas with elevated heat flow, may demonstrate LST anomalies. The analysis is done based on multiple images from the years between 2016 and 2021. Initially, we tried to use both winter and summer time series of Landsat images to acquire information on thermal characteristics of the land surface, however, wintertime series did not seem to add any significant information nor to give any substantial result. This indifference might be due to the nature of thermal manifestations that exist in our study area, and to the fact that they are very limited in space and does not cover wide noticeable areas.

In this paper, we present the results of the application of Landsat 8 derived LST in the exploration for geothermal anomalies in NE Morocco. In view of the uncertainties of satellite LST, the following results of the present work should be evaluated thoughtfully. Many factors can actually affect remotely sensed LST such as moisture availability (which we carefully checked while working on this paper and it did not show any clear impact), evapotranspiration, rainfall and fire events, but also pre-seismic and volcanic activity, which can eventually cause spatiotemporal LST anomalies.

Usually, soil moisture can be a major factor in developing weather patterns and producing precipitation. Many studies agreed on the fact that surface soil moisture, temperature and vegetation are connected and that soil moisture strongly disturbs the amount of precipitation that runs off into nearby streams and rivers and this affects the surface temperature eventually. However, collected data to calculate soil moisture within our study area has been less significant and plots the latter in the dry level, furthermore, the spatiotemporal variation of the soil moisture index between the years 2016 and 2021 seems to be unrelated to the land surface temperature.

Based on geophysical studies carried out by Geoatlas between 2000 and 2002, the Liassic reservoir exists within the limits between the Triffa basin in the North and Beni Snassen Mountains in the South (Figure 2) and a NE-SW major fault (Figure 5) separates the Lias into two sections: 1) a northern section where the Lias sinks deeply, and gets completely isolated in recharge zones; 2) a southern section where the Liassic reservoir is captive and connected to its outcrops at the Beni Snassen level. Generally, the recharge zone is located in Beni Snassen. Triffa basin is divided to three blocks: i) one block is characterized by a flow towards the N and NE towards Algeria where the aquifer continues; ii) another block (Fezouane block) is characterized by deep water circulations and high temperature degrees; iii) the third block is the Berkane block and is characterized by a radial flow mainly around the municipality of Berkane (Barkaoui et al., 2014).

With the fractures pattern dominated by a NE-SW system ranging from N40 to N70, a N-S system ranging from N10 to N45 and an EW to WNW-ESE systems ranging from N80 to N120 (Redouane et al., 2022a), most of the faults are located in Kebdana, Amejjaou, Nador and Melilla regions (Figure 5). According to many other studies (i.e. Ait brahim and chotin, 1990), recent volcanic activity in NE of Morocco is assumed to be related to the NE-SW flow causing hydrothermal alteration of rocks.

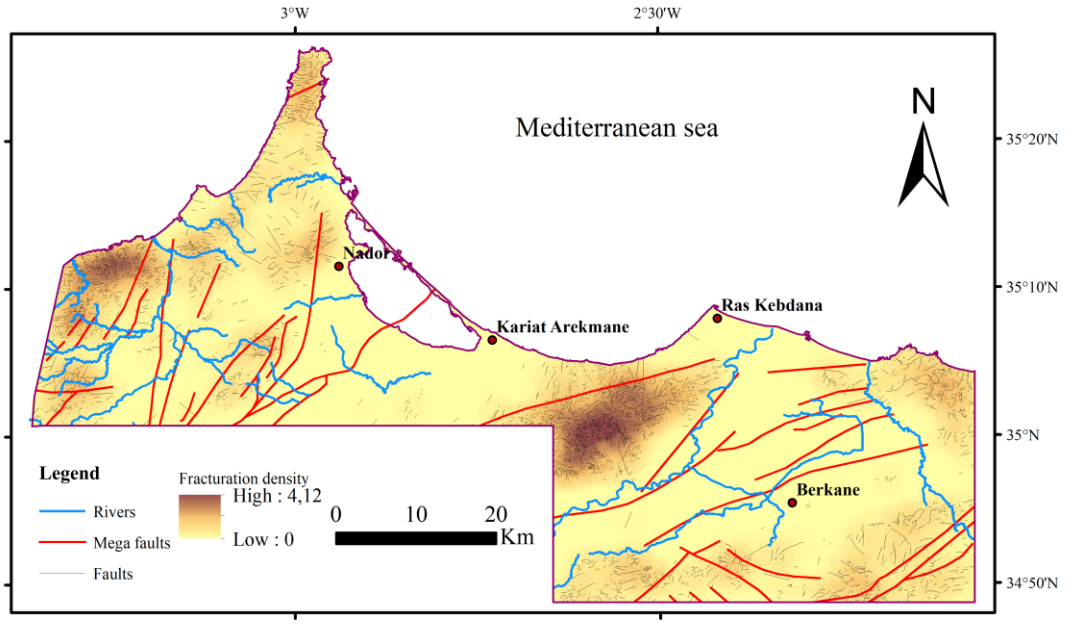

Figure 5: fault density map of NE Morocco

Mineral alteration analysis of hydrothermal minerals in basaltic rocks supports the involvement of at least two different hydrothermal fluids, a low temperature fluid and a high temperature fluid (Redouane et al., 2022b). The hottest geothermal manifestation within the study area is located in the southeast of Nador, close to Kariat Arekmane village (Figure 6) where the water is Cl-Na rich and has a surface temperature ranging between 42 and 43 °C (Table 4). Passing from the north to the southeastern parts, close to Berkane and Oujda, thermal waters' nature become HCO3-Ca rich and shows lower temperatures at the surface (Figure 2 and Table 4).

Table 4: Measured temperature data and main geochemical prints of thermal manifestations within the study area

NOM	IRE	Tmean(°C)	CHIMICAL FACIES
LALLA CHAFFIA	101/10	30	HCO_3 -Na & SO_4 -(Mg)
AIN MESSAOUDA		19	Cl -Na & -(SO_4 -Ca-Mg)
HAMMAM BENI SIDEL		34	Cl -Na & -HCO_3 -Na
IN HADDOU OU HAMMA	1604/6	28	Cl -Na
HAMMAM-CHAUD	1605/6	38,5	Cl -Na
YADIN	1619/6	43	Cl -Na
KARIAT AREKMAN		42	Cl -Na
AINAOULLOU		23	-HCO_3-Ca
SOURCE DE KISS		25	Cl -Na
AINCHOUN	1279/7	29	HCO_3-Ca
AIN REGADA.V	770/7	29,5	HCO_3-Ca
1267/6	1267/7	34,5	HCO_3-Ca
FEZZOUANE	1268/7	37	HCO_3-Ca
SIDI RAHMOUN	1274/7	29	HCO_3-Ca

Results are presented on LST maps in figure 6 and temperatures are classified using the classification of (AlaviPanah et al., 2017), which consists of the use of mean temperature (Tmean) and standard deviation (STD) (Table 5). Notwithstanding the differences

between MODIS daytime LST and Landsat 8 (OLI/TIRS) LST, they generally have correlated positively in the present work (Figure 6, 7). Compared to MODIS LST, Landsat shows lower values ~ -1.1 °C. Another factor to take into account is that remotely sensed LST from both Landsat and MODIS is acquired only during cloud free days so it does not reflect the same exact climate conditions within the study area, but they remain the most reliable data source for many for the purpose of this work, where we try to detect areas with high thermal anomalies. With the help of geological data including geological and structural maps as well as measured temperature data from the hot springs and boreholes, we were able to interpret the geothermal anomalies results and identify geothermal areas.

Table 5: Application of Surface Temperature Classification of AlaviPanah et al., 2017 showing corresponding temperature range for this study

LST Class	Class Range	Temperature range
Very low temperature	$T \leq Tmean - 1.5\ STD$	31,34
Low temperature	$Tmean - 1.5STD < T \leq Tmean - STD$	32,95
Medium temperature	$Tmean - STD < T \leq Tmean$	36,18
High temperature	$Tmean < T \leq Tmean + STD$	39,40
Very high temperature	$Tmean + STD < T \leq Tmean + 1.5\ STD$	41,01
Extremely high temperature Class	$T > Tmean + 1.5\ STD$	>41

The comparison of Landsat 8 derived LST in the study area with MODIS daytime LST (Figure 6 and 7) shows a general coherence in terms of high and low thermal areas, with a noticeable increase from the coast towards the land and the Foreland Mountains. While comparing Landsat 8 derived LST with air temperature data from weather stations, operating in NE of Morocco (Table 3), shows that calculated LST is generally reliable as it respects the average of the mean measured Temperatures from the different weather stations covering the area in question.

Table 6 presents extracted mean temperatures during the years between 2016 and 2021, together with the max temperature, the min temperature and standard deviation. It shows that the warmest year was 2021 and the coldest was 2016. The choice of the classification that uses mean temperatures was made to avoid any unwanted effects and to keep the comparison stands right regardless of the slight variations that might occur while adapting different legends.

Table 6: Land surface temperatures from map data and standard of variation for the study years.

Years	T mean	Tmax	Tmin	STD
2016	33,52	42,3	20,7	2,7
2017	33,75	43,18	20,8	3,26
2018	37,61	48,04	19,78	3,59
2019	35,82	44,9	19	3,09
2020	38,57	47,42	22,7	2,92
2021	37,78	47,8	21,7	3,78
Mean	**36,18**	45,61	20,78	**3,22**

Apart from the years of 2016 and 2017 (Figure 6a, 6b), where areas with thermal springs are considered as cold areas based on LST derived maps, geothermal manifestations generally are represented within warm areas. The highest temperature values of hot springs

and at the surface of boreholes are found in the North and the NE parts of the study area, mainly in Kariat Arekmane in the SE of Nador city and Fezouane in the east of Berkane city (Figure 6c, 6d, 6e, 6f).

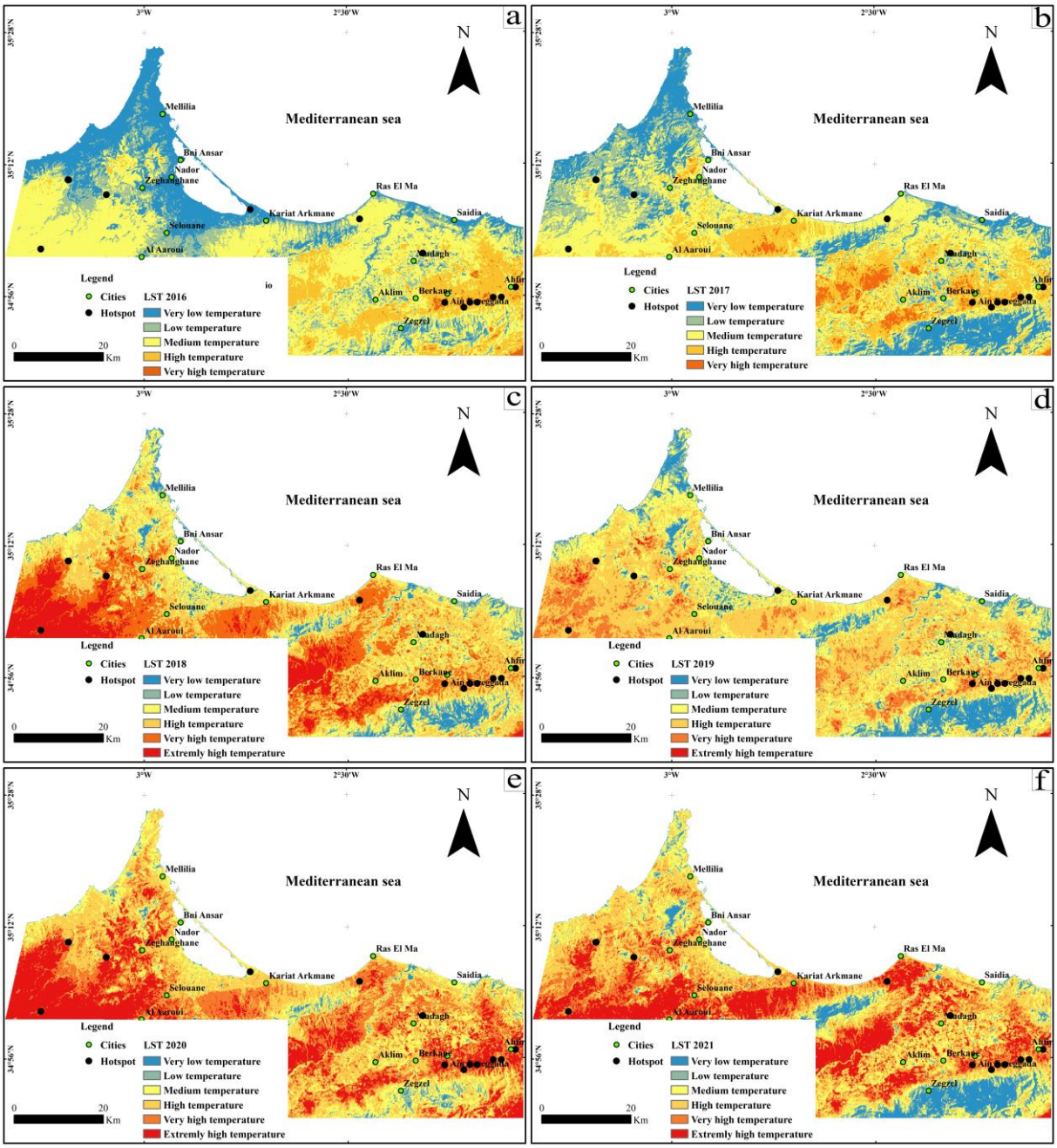

Figure 6: Summer time LST (2016 – 2021) for NE of Morocco

LST mapping results show that areas with high thermal anomalies are mostly located in the eastern foreland namely in Kebdana, Ghareb and the North of Beni Snassen Mountains (Figure 2 and 6). Towards the north of Beni Snassen, LST shows high to very high temperatures according to the adopted classification (Table 5), whereas the rest of the Mountain is considered as the coldest, and it is in the northeastern part of it, close to the right to Berkane city where most of hot springs outcrop. Kebdana and Ghareb show high land surface temperatures as well, but due to the largeness of the area, the outcome does not seem to be very instructive, nor does it point out exactly spots with the highest geothermal potential.

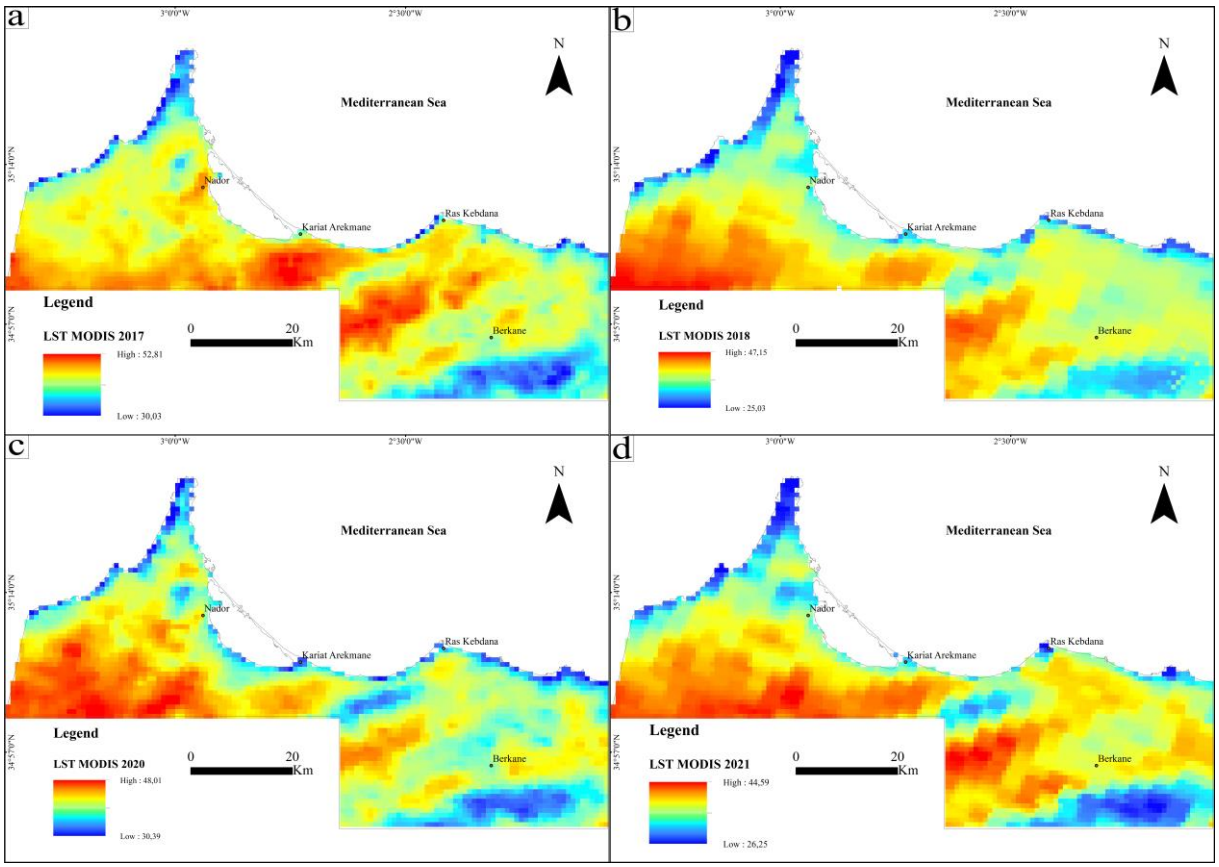

Figure 7: MODIS LST (2017-2018-2020-2021) maps for NE of Morocco

Recent magmatic activity in our study area (Neogene-Quaternary) works as a heat source for the geothermal system and the faulting pattern provides thermal pathways for the heat transfer. Based on the compilation of all the data, three geothermal cities (Berkane, Ahfir and Ras El ma) and three promising landmasses (Kebdana-Beni Snassen, Nador and its surrounding satellites and the Ghareb plain) were highlighted in the southern half of the study area.

The closest study of the current work has been done recently (El Morabit et al., 2021), where authors worked on extracting spectral index from Landsat 8 (OLI/TIRS) to detect geothermal anomalies in a small area covering Berkane and Ahfir. Calculated temperatures based on their study range between 29.67 and 46.45 °C and the highest temperature value is found in the east of Berkane. The study does not include any further details, however, it insists on the effectiveness of the method on detecting thermal anomalies and approves of Berkane-Ahfir as an area with high geothermal potential.

To summarize, TIR remote sensing has proven to be, in general terms, an effective and reliable method for early phases of geothermal exploration. The method applied in this study helps to reduce the cost and time engaged to explore areas with thermal manifestations, however, it requires a thorough support from all possible resources and available data from geology and geophysics.

5. CONCLUSIONS

This work presents the results of the analysis of Landsat 8 derived LST time series data with the aim of highlighting areas with high geothermal anomalies, which might serve as potential geothermal sites for further exploration.

As far as we got from the application of remote sensing using Landsat 8 (OLI/TIRS) for the purpose of detecting geothermal anomalies, we conclude that it is generally worthy, however the results are limited. The limitation of the application might be due to the largeness of the study area, or to the inability to build up an advanced level of contrast that allows slight differences to be detected as Landsat 8 bands` spatial resolution remains relatively high. This might also be the reason for the inadequacy of winter LST values with the aim of this study, as areas with higher temperatures are notably large with no clear limits. However, this work might suggest that there are areas with geothermal potential still unexplored, mainly in the foreland units, which must be evaluated as possible sites of geothermal interest, and where future exploration should focus on. Especially that even earlier studies on heat flow density and

geothermal gradients assume that NE of Morocco is currently having an active geothermal system and has the highest geothermal gradients and heat flux.

According to this study and data from other studies, the presence of hydrothermal alteration, high land surface temperatures, hot springs and lineaments in Nador-Berkane region indicates a high geothermal potential. Thus, it is permissible to speak about three promising landmasses with high geothermal potential, which are Berkane, Nador and Ghareb.

REFERENCES

Afrasiabi Gorgani, S., Panahi, M., Rezaie, F. (2013). The Relationship between NDVI and LST in the urban area of Mashhad, Iran. International Conference on Civil Engineering Architecture & Urban Sustainable Development, (December), 1–17.

Aït Brahim, L. and Chotin, P. (1990). Oriental Moroccan Neogene Volcanism and Strike-Slip Faulting. Journal of African Earth Sciences (and the Middle East), 11, 273-280. https://doi.org/10.1016/0899-5362(90)90005-Y

Alavipanah, S.K., Mogaddam, M.K., Firozjaei, M.K. (2017). Monitoring spatiotemporal changes of heat island in Babol city due to land use changes. International Archives of the Photogrammetry, Remote Sensing and Spatial Information Sciences - ISPRS Archives, 42(4W4), 17–22.

Barkaoui, A.E. (2014). La province géothermique du Maroc Nord Oriental : Hydrogéochimie, Modélisation analytique, Paléoclimat, SIG et valorisation énergétique. Thèse en Géosciences. Faculté des sciences, Université Mohammed premier, Oujda.

Barkaoui, A.E., Zarhloule, Y., Rimi, A., Boughriba, M., Verdoya, M., Bouri, S. (2013). Hydrogeochemical investigations of thermal waters in the northeastern part of Morocco. Journal of Environmental Earth Sciences. https://doi.org/10.1007/s12665-013-2582-x.

Chan, H.P., Chang, C.P., Dao, P.D. (2018). Geothermal Anomaly Mapping Using Landsat ETM+ Data in Ilan Plain, Northeastern Taiwan. Pure Appl. Geophys. 175, 303–323. https://doi.org/10.1007/s00024-017-1690-z.

Coulon, C., Megartsi, M., Fourcade, S., Maury, R.C., Bellon, H., Louni-Hacini, A., Cotton, J., Hermitte, D. (2002). Post-collision transition from calc-alkaline to alkaline volcanism during the Neogene in Oranie (Algeria): magmatic expression of a slab breakoff, Lithos. 62, 87–110.

Donglian, S.M.K. (2007). Note on the NDVI-LST relationship and the use of temperature-related drought indices over North America. Geophysical Research Letters, 34(24).

El Azzouzi, M., Bernard-Griffiths, J., Bellon, H., Maury, R.C., Pique, A., Fourcade, S., Cotten, J., Hernandez J. (1999). Evolution des sources du volcanisme marocain au cours du Néogène. C. R. Acad. Sci., Paris, 329, II, 95-102.

El Morabit, I., Maimouni, S., Fekri, A. (2021). Geothermal potential mapping of Northeast Morocco (Bekrane Ahfir) using remote sensing data and GIS. E3S Web of Conferences. 234. 00093. https://doi.org/10.1051/e3sconf/202123400093.

Freitas, S.C.S.C., Trigo, I.F., Macedo, J., Barroso, C., Silva, R., Perdigao, R., Perdigão, R. (2013). Land surface temperature from multiple geostationary satellites. International Journal of Remote Sensing, 34(9–10), 3051–3068.

Gemitzi, A., Dalampakis, P., Falalakis, G. (2021). Detecting geothermal anomalies using Landsat 8 thermal infrared remotely sensed data. International Journal of Applied Earth Observation and Geoinformation. https://doi.org/10.1016/j.jag.2020.102283.

Hernandez, J., Bellon, H. (1985). Chronologie K-Ar du volcanisme miocène du Rif oriental (Maroc) : implications tectoniques et magmatologiques. Rev Géol Dyn Géogr Phys 26, 85-94.

Khalis, H., Sadiki, A., Jawhari, F., Mesrar, H., Azab, E., Gobouri, A.A., Adnan, M., Bourhia, M. (2021). Effects of Climate Change on Vegetation Cover in the Oued Lahdar Watershed. Northeastern Morocco. Plants, 10(8), 1624.

Mattauer, M., Tapponnier, P. and Proust, F. (1977). Sur les mécanismes de formation des chaînes intracontinentales. L'exemple des chaînes atlasiques du Maroc. Bulletin de la Société Géologique de France, S7-19, 521-526. https://doi.org/10.2113/gssgfbull.S7-XIX.3.521.

Maury, R.C., Fourcade, S., Coulon, C., El Azzouzi, M., Bellon, H., Coutelle, A., Ouabadi, A., Semroud, B., Megartsi, M., Cotton, J., Belanteur, O., Louni-Hacini, A., Pique, A., Capdevila, R., Hernandez, J. and Rehault, J.P. (2000). Post-Collisional Neogene Magmatism of the Mediterranean Maghreb Margin: A Consequence of Slab Breakoff. Comptes Rendus de l'Académie des Sciences, 331, 159-173. https://doi.org/10.1016/S1251-8050(00)01406-3.

Missenard, Y., Zeyen, H., Frizon de Lamotte, D., Leturmy, P., Petit, C., Sebrier, M. and Saddiqi, O. (2006). Crustal versus Asthenospheric Origin of Relief of the Atlas Mountains of Morocco. Journal of Geophysical Research, 111, Article ID: B03401. https://doi.org/10.1029/2005JB003708.

Rakus, M. (1979). Evolution et position paléogéographique des Monts d'Oujda au cours du Mésozoïque. Mines, Géologie et Energie, 46, 75–78.

Redouane, M., Haissen, F., Cong, Z., Sadki, O., Raji, M. (2022b). Plio-Quaternary Volcanism in Northeastern Morocco: Petrography and Geochemistry of Outcrops with High Geothermal Potential. Open Journal of Geology, 12, 829-869. https://doi:10.4236/ojg.2022.1211040.

Redouane, M., Si Mhamdi, H., Haissen, F., Raji, M., Sadki, O. (2022a). Lineaments Extraction and Analysis Using Landsat 8 (OLI/TIRS) in the Northeast of Morocco. Open Journal of Geology, 12, 333-357. https://doi.org/10.4236/ojg.2022.125018.

Rimi, A. (1999). Variations régionales du flux géothermique au Maroc, application. Thèse de Doctorat des Sciences, Univ. Mohammed V, Fac Sci Rabat.

Romaguera, M., Vaughan, R.G., Ettema, J., Izquierdo-Verdiguier, E., Hecker, C.A., van der Meer, F.D. (2017). Detecting geothermal anomalies and evaluating LST geothermal component by combining thermal remote sensing time series and land surface model data. Remote Sensing of Environment, S0034425717304649. https://doi.org/10.1016/j.rse.2017.10.003.

Ronald, B.S. (2005). Computing the Planck Function., Yale University.

Suter, G. (1980). Carte structurale de la chaîne rifaine à 1/500000. Notes et Mémoires du Service Géologique du Maroc. 245.

Tucker, G., Gasparini, N., Lancaster, S., Bras, R. (1997). An Integrated Hillslope and Channel Evolution Model as an Investigation and Prediction Tool. Department of Civil and Environmental Engineering Massachusetts Institute of Technology.

Van der Meer, F., Hecker, C., Van Ruitenbeek, F., Van der Werff, H., De Wijkerslooth, C., Wechsler, C. (2014). Geologic remote sensing for geothermal exploration: A review. International Journal of Applied Earth Observation and Geoinformation, 33, 255–269. https://doi.org/10.1016/j.jag.2014.05.007.

Zarhloule, Y., Rimi, A., Boughriba, M., Barkaoui, A.E., Lahrach, A. (2010). The geothermal research in Morocco: history of 40 years. In proceedings of the World Geothermal Congress (2010).